Relativistic two fluid plasmas in the vicinity of a Schwarzschild black hole—Local approximation. II

V. Buzzi and K. C. Hines
School of Physics, University of Melbourne, Parkville, Victoria 3052, Australia

R. A. Treumann
Max-Planck-Institut für Extraterrestrischephysik, Garching bei München, Germany
(Received 12 May 1994)

The 3 + 1 split of general relativity is used in a preliminary investigation of waves propagating in a plasma influenced by the gravitational field of a Schwarzschild black hole. The relativistic two fluid equations have been reformulated, as explained in an earlier paper, to take account of gravitational effects due to the event horizon. Here, a local approximation is used to investigate the one-dimensional radial propagation of longitudinal waves. A study is also included of the two-stream instability in view of its importance in astrophysics. Dispersion relations are obtained for these waves and solved numerically for the wave number k.

PACS number(s): 95.30.Qd, 95.30.Sf, 97.60.Lf

I. INTRODUCTION

In the preceding paper [1] a local approximation has been used to obtain dispersion relations for the Alfvén and high frequency electromagnetic waves existing in the vicinity of a Schwarzschild black hole. The present paper is concerned with the investigation of longitudinal waves and the two-stream instability in this environment. A general introduction to plasma physics in the presence of the gravitational field of a black hole has been presented in the preceding paper (paper I) where also the desirability of employing the 3 + 1 formulation of general relativity of Thorne *et al.* [2,3] is discussed.

In the present paper a general relativistic version of the two-fluid formulation of plasma physics is again considered using the 3 + 1 formalism. A linearized treatment of plasma waves is developed, in analogy with the special relativistic formulation by Sakai and Kawata [4] (SK), and used to investigate the nature of the waves close to the horizon of a Schwarzschild black hole. Whereas in paper I transverse electromagnetic waves were investigated using the linearized two fluid equations, in this paper longitudinal waves, together with the two-stream instability, are studied.

The two-stream instability can be treated as an extension of the equations for the longitudinal waves. The analytic results obtained for these waves are general in that they apply equally to either an electron-positron plasma or to an electron-ion plasma. The two-stream instability has long been regarded as important because of its likely involvement in the emission mechanism responsible for the observed radiation from pulsars. It could also be important in understanding emission from black holes. The history of the two-stream instability is interesting in that, as far as the authors are presently aware, there exists no correct formulation for the relativistic two-stream instability in the published literature. The nonrelativistic two-stream instability has been investigated by a number of authors and is a well-understood phenomenon.

Historically, there has been strong disagreement as to the occurrence, or otherwise, of the two-stream instability in a relativistic plasma and as to whether it could be important for understanding the problem of pulsar radiation emission. Lominadze and Mikhailovskii [5] discussed the importance of the two-stream instability for pulsar emission theories. They showed that longitudinal waves with a phase velocity lower than that of light can exist in a relativistic plasma and further, that these waves are self-damping and can be excited by fast particle beams. They also showed that the two-stream instability can, in fact, occur for phase velocities lower than that of light. Earlier, Goldreich and Julian [6] had demonstrated the flow of plasma streams along the field lines and Buti [7,8] investigated the two-stream instability using a kinetic approach including some relativistic effects. Attempts have been made in the past to find a solution including a heuristic guess at a dispersion relation made by Finkelstein and Sturrock [9] which is incorrect. Sakai and Kawata [4] quote a result, using a two-fluid approach, but give no account of how they arrived at their result and, in fact, their dispersion relation is also incorrect, although they do note the importance of the two-stream instability for the pulsar problem. A correct two-fluid calculation of the special relativistic dispersion relation, by Cornish [10], does exist but remains, as yet, unpublished.

The reader is referred to Sec. II in paper I for a summary of the 3 + 1 formulation of general relativity relevant to the Schwarzschild metric. In the present paper Sec. II presents the set of nonlinear two fluid equations expressing continuity and the conservation of energy and momentum in which the two fluids are coupled together via Maxwell's equations. Section III begins with a brief summary of the dependence of the unperturbed field and

fluid parameters on the radial coordinate z as would be required for the study of the longitudinal modes and contains the linearized one-dimensional continuity and Poisson equations together with the longitudinal component of the momentum equation.

In analyzing the dispersion relations the local approximation is used in precisely the manner described in Sec. VI of paper I. Section IV of the present paper deals with the derivation of the dispersion relation for the longitudinal waves. Section V discusses the adaptation of the longitudinal dispersion relation treatment to the special and more complicated case of the two-stream instability.

The numerical procedure for determining the roots of the dispersion relations is reviewed briefly in Sec. VI and the appropriate form of the longitudinal equations are quoted. The numerical solutions for the wave number k are presented in Sec. VII for the longitudinal waves and in Sec. VIII for the two-stream instability.

II. LONGITUDINAL TWO FLUID EQUATIONS

The reader is referred to paper I for a derivation of the fundamental nonlinear two fluid equations in their $3+1$ form. Maxwell's equations in 3+1 form are also presented in paper I. Only a summary of the two fluid equations relevant to the longitudinal waves will be restated here.

As in paper I, the notation adopted throughout will be that used by Thorne, Price, and Macdonald [2] (TPM). In general, $G = c = k_B = 1$, cgs units will be used and all equations are valid in a fiducial observer (FIDO) rest frame (at rest with respect to the Schwarzschild coordinates). The fluid and field parameters are defined as follows: n_s is the fluid density, v_s is the fluid velocity, the pressure is defined by P_s, charge is given by q_s, ε_s is the internal energy density, and γ_s is the relativistic Lorentz factor. The electric and magnetic fields are given by $\mathbf{E}$ and $\mathbf{B}$, respectively. The lapse function is defined by α as in paper I and the acceleration is defined again as $\mathbf{a} = -(1/\alpha)\nabla\alpha$. In its 3+1 form, the continuity equation for each of the fluid species is given by

$$\frac{\partial}{\partial t}(\gamma_s n_s) + \nabla\cdot(\alpha\gamma_s n_s \mathbf{v}_s) = 0\,, \tag{1}$$

where s is the species index, 1 for electrons and 2 for positrons (or ions). With Maxwell's equations, as given in paper I, coupling each single fluid of species s to the electromagnetic fields, the energy and momentum conservation equations may be written as follows for each species s:

$$\frac{1}{\alpha}\frac{\partial}{\partial t}P_s - \frac{1}{\alpha}\frac{\partial}{\partial t}\left[\gamma_s^2(\varepsilon_s + P_s)\right] - \nabla\cdot\left[\gamma_s^2(\varepsilon_s + P_s)\mathbf{v}_s\right] + \gamma_s q_s n_s \mathbf{E}\cdot\mathbf{v}_s + 2\gamma_s^2(\varepsilon_s + P_s)\,\mathbf{a}\cdot\mathbf{v}_s = 0 \tag{2}$$

and

$$\gamma_s^2(\varepsilon_s + P_s)\left(\frac{1}{\alpha}\frac{\partial}{\partial t} + \mathbf{v}_s\cdot\nabla\right)\mathbf{v}_s + \nabla P_s - \gamma_s q_s n_s(\mathbf{E} + \mathbf{v}_s\times\mathbf{B}) + \mathbf{v}_s\left(\gamma_s q_s n_s \mathbf{E}\cdot\mathbf{v}_s + \frac{1}{\alpha}\frac{\partial}{\partial t}P_s\right) + \gamma_s^2(\varepsilon_s + P_s)\left[\mathbf{v}_s(\mathbf{v}_s\cdot\mathbf{a}) - \mathbf{a}\right] = 0\,. \tag{3}$$

Poisson's equation takes the form

$$\nabla\cdot\mathbf{E} = 4\pi\sigma, \tag{4}$$

where the charge density is defined as

$$\sigma = \sum_s \gamma_s q_s n_s\,. \tag{5}$$

Recall from paper I that the fluid velocities and fields are all fiducial observer (FIDO) measured quantities whereas the fluid densities and pressures are measured in the comoving fluid rest frame. If, now, one sets the lapse function α to unity so that the acceleration goes to zero (the limit of zero gravity), these equations reduce to the corresponding special relativistic fluid equations given by SK [4], even though the equations in the case considered here are valid in a FIDO frame and the special relativistic equations of SK [4] are valid in a frame in which both fluids are at rest.

The Rindler coordinate system in which space is locally Cartesian is used here as in paper I. The Rindler metric provides a good approximation to the Schwarzschild metric close to the black hole horizon. The essential features of the horizon and the $3+1$ split are retained without the complication of explicitly curved spatial three-geometries. Recall from paper I that the Schwarzschild metric is approximated in Rindler coordinates by

$$ds^2 = -\alpha^2 dt^2 + dx^2 + dy^2 + dz^2\,, \tag{6}$$

where

$$x = 2M\left(\theta - \frac{\pi}{2}\right)\,,\quad y = 2M\phi\,,\quad z = 4M\left(1 - \frac{2M}{r}\right)\,. \tag{7}$$

A discussion of the transformation from the Schwarzschild metric to the Rindler metric can be found in the work of TPM [3]. The standard lapse function, $(1 - r_H/r)^{1/2}$, is again denoted by α which simplifies in Rindler coordinates to $z/2r_H$, where r_H is the Schwarzschild radius.

III. LINEARIZED EQUATIONS

Consideration in the present paper is again restricted to one-dimensional wave propagation in the radial z direction as explained previously in Sec. IV of paper I.

A. Dependence of unperturbed values on z

The dependences of the unperturbed equilibrium quantities on z are summarized below. Because the fluid elements are in a region close to the black hole horizon, the unperturbed radial velocity for each species as measured by a FIDO, along $\mathbf{e}_{\hat{z}}$, as in paper I, is assumed to be the freefall velocity so that

$$u_{0s}(z) = v_{\rm ff}(z) = \left[1 - \alpha^2(z)\right]^{\frac{1}{2}} . \tag{8}$$

With $v_{\rm ff} = (r_H/r)^{\frac{1}{2}}$, the number density for each species can be written as

$$n_{0s}(z) = n_{Hs} v_{\rm ff}^3(z) . \tag{9}$$

From Eq. (9), the pressure for each fluid species may be written in terms of the freefall velocity as

$$P_{0s}(z) = P_{Hs} v_{\rm ff}^{3\gamma_g}(z) . \tag{10}$$

Since $P_{0s} = k_B n_{0s} T_{0s}$ then it follows that, with $k_B = 1$,

$$T_{0s} = T_{Hs} v_{\rm ff}^{3(\gamma_g - 1)}(z) . \tag{11}$$

Since the unperturbed magnetic field has been chosen to be purely in the radial z direction, it is also parallel to the infall fluid velocity $u_{0s}(z)\mathbf{e}_{\hat{z}}$ for each fluid. Along with the infall fluid velocity, it thus does not experience effects of spatial curvature. The dependence of the magnetic field on the radial coordinate r is due entirely to flux conservation. Recall from paper I that the unperturbed magnetic field may be written in terms of the freefall velocity as

$$B_0(z) = B_H v_{\rm ff}^4(z) . \tag{12}$$

The derivatives, with respect to z, of the unperturbed field and fluid quantities are directly proportional to the derivative of the freefall velocity with respect to z. Hence, since

$$\frac{dv_{\rm ff}}{dz} = -\frac{\alpha}{2r_H}\frac{1}{v_{\rm ff}} , \tag{13}$$

it follows that

$$\frac{du_{0s}}{dz} = -\frac{\alpha}{2r_H}\frac{1}{v_{\rm ff}} , \quad \frac{dB_0}{dz} = -\frac{4\alpha}{2r_H}\frac{B_0}{v_{\rm ff}^2}$$
$$\frac{dn_{0s}}{dz} = -\frac{3\alpha}{2r_H}\frac{n_{0s}}{v_{\rm ff}^2} , \quad \frac{dP_{0s}}{dz} = -\frac{3\alpha}{2r_H}\frac{\gamma_g P_{0s}}{v_{\rm ff}^2} . \tag{14}$$

B. Linearized longitudinal wave equations

Recall from paper I that the linearized continuity equation is given by

$$\gamma_{0s}\left(\frac{\partial}{\partial t} + u_{0s}\alpha\frac{\partial}{\partial z} + \frac{u_{0s}}{2r_H} + \gamma_{0s}^2\alpha\frac{du_{0s}}{dz}\right)\delta n_s + \left(\alpha\frac{\partial}{\partial z} + \frac{1}{2r_H}\right)(n_{0s}\gamma_{0s}u_{0s})$$
$$+ n_{0s}\gamma_{0s}^3\left[u_{0s}\frac{\partial}{\partial t} + \alpha\frac{\partial}{\partial z} + \frac{1}{2r_H} + \alpha\left(\frac{1}{n_{0s}}\frac{dn_{0s}}{dz} + 3\gamma_{0s}^2 u_{0s}\frac{du_{0s}}{dz}\right)\right]\delta u_s = 0 . \tag{15}$$

Similarly, the longitudinal component of the equation for the conservation of momentum, as derived in paper I, is given by

$$\left\{\frac{\partial}{\partial t} + \alpha u_{0s}\frac{\partial}{\partial z} + \alpha\gamma_{0s}^2\left(1 + u_{0s}^2\right)\frac{du_{0s}}{dz}\right\}\delta u_s - \frac{\alpha q_s n_{0s}}{\rho_{0s}\gamma_{0s}}\delta E_z$$
$$+ \frac{1}{\gamma_{0s}^2 n_{0s}}\left\{\frac{\gamma_{0s}^2\gamma_g P_{0s}}{\rho_{0s}}\left(\alpha\frac{\partial}{\partial z} + u_{0s}\frac{\partial}{\partial t}\right) + \alpha\gamma_{0s}^2\frac{\gamma_g P_{0s}}{\rho_{0s}}\left(\frac{1}{P_{0s}}\frac{dP_{0s}}{dz} - \frac{1}{n_{0s}}\frac{dn_{0s}}{dz}\right)\right.$$
$$\left. + \left(1 + \frac{\gamma_{0s}^2\gamma_g P_{0s}}{\rho_{0s}}\right)\left(u_{0s}\gamma_{0s}^2\alpha\frac{du_{0s}}{dz} + \frac{1}{2r_H}\right)\right\}\delta n_s + \left(u_{0s}\alpha\frac{du_{0s}}{dz} + \frac{\alpha}{\rho_{0s}}\frac{dP_{0s}}{dz} + \frac{1}{\gamma_{0s}^2 2r_H}\right) = 0 . \tag{16}$$

The linearized Poisson equation is

$$\frac{\partial\delta E_z}{\partial z} = 4\pi e(n_{02}\gamma_{02} - n_{01}\gamma_{01}) + 4\pi e(\gamma_{02}\delta n_2 - \gamma_{01}\delta n_1)$$
$$+ 4\pi e(n_{02}u_{02}\gamma_{02}^3\delta u_2 - n_{01}u_{01}\gamma_{01}^3\delta u_1) . \tag{17}$$

IV. LONGITUDINAL WAVE DISPERSION RELATION

In order to derive the dispersion relation for the longitudinal wave modes, a combination of the linearized longitudinal force equation, Eq. (16), the linearized con-

tinuity equation, Eq. (15), and the linearized Poisson's equation, Eq. (17), is used. In the local approximation for α, as detailed in paper I, the medium near the black hole is divided into thin concentric layers, each of which is centered around a particular value $z = z_0$ in the one-dimensional treatment. The approximation $\alpha \simeq \alpha_0$ is valid within a particular layer, where α_0 is the local, or "mean-field," value of α. Therefore, the unperturbed field and fluid quantities and their derivatives, which are functions of α, take on their corresponding "mean-field" values for a given α_0. Hence, the coefficients in Eqs. (16), (15), and (17) become essentially constant within each layer, evaluated at each fixed mean-field value, $\alpha = \alpha_0$.

Because the coefficients in the linearized equations are no longer z dependent within each layer, it is possible to Fourier transform the equations with respect to z, assuming plane-wave-type solutions for the perturbations of the form $\sim e^{i(kz-\omega t)}$ for each α_0 layer. In this approximation, Fourier transforming Eq. (15) gives the following for each species s:

$$\delta n_s = -n_{0s}\gamma_{0s}^2 \left\{ \frac{\alpha_0 k - \omega u_{0s} - i\alpha_0(Dn_{0s}/n_{0s} + 3u_{0s}\gamma_{0s}^2 Du_{0s}) - i/2r_H}{\alpha_0 k u_{0s} - \omega - i(u_{0s}/2r_H + \alpha_0\gamma_{0s}^2 Du_{0s})} \right\} \delta u_s, \tag{18}$$

where the derivatives of the unperturbed fields and fluid quantities, evaluated for each $\alpha = \alpha_0$, are given by

$$Du_{0s} = \left.\frac{du_{0s}}{dz}\right|_{\alpha=\alpha_0}, \quad Dn_{0s} = \left.\frac{dn_{0s}}{dz}\right|_{\alpha=\alpha_0},$$
$$DP_{0s} = \left.\frac{dP_{0s}}{dz}\right|_{\alpha=\alpha_0}, \quad DB_0 = \left.\frac{dB_0}{dz}\right|_{\alpha=\alpha_0}. \tag{19}$$

Fourier transforming Poisson's equation, Eq. (17), leads to

$$ik\delta E_z = 4\pi e(\gamma_{02}\delta n_2 - \gamma_{01}\delta n_1) + 4\pi e(n_{02}u_{02}\gamma_{02}^3\delta u_2 - n_{01}u_{01}\gamma_{01}^3\delta u_1). \tag{20}$$

Finally, the longitudinal part of the force equation, Eq. (16), when Fourier transformed, gives

$$(\alpha_0 k u_{0s} - \omega - i\alpha_0\gamma_{0s}^2(1+u_{0s}^2)Du_{0s})\delta u_s + \frac{1}{\gamma_{0s}^2 n_{0s}}\left\{\gamma_{0s}^2\frac{\gamma_g P_{0s}}{\rho_{0s}}\left(\alpha_0 k - \omega u_{0s}\right) - i\alpha_0\gamma_{0s}^2\frac{\gamma_g P_{0s}}{\rho_{0s}}\right.$$
$$\left.\times\left(\frac{1}{P_{0s}}DP_{0s} - \frac{1}{n_{0s}}Dn_{0s}\right) - i\left(1 + \frac{\gamma_{0s}^2\gamma_g P_{0s}}{\rho_{0s}}\right)\left(\alpha_0\gamma_{0s}^2 u_{0s}Du_{0s} + \frac{1}{2r_H}\right)\right\}\delta n_s + \frac{i\alpha_0 q_s n_{0s}}{\rho_{0s}\gamma_{0s}}\delta E_z = 0. \tag{21}$$

From Eqs. (18), (20), and (21) the dispersion relation for the longitudinal wave modes can be evaluated.

Substituting from Eqs. (18) and (20) into Eq. (21), one can eliminate the density perturbations δn_1 and δn_2 and the field perturbation δE_z in terms of the velocity perturbations δu_1 and δu_2, resulting in a set of two coupled equations which lead to the following dispersion relation for the longitudinal waves:

$$1 = \frac{\alpha_0}{k}\sum_s \frac{\omega_{ps}^2}{\gamma_{0s}^2}\left[\alpha_0 k - \frac{i}{2r_H} - i\alpha_0\gamma_{0s}^2\left(\frac{1}{n_{0s}}Dn_{0s} + 2\gamma_{0s}^2 u_{0s}Du_{0s}\right)\right]$$
$$\times\left\{\left[\alpha_0 k u_{0s} - \omega - i\alpha_0\gamma_{0s}^2(1+u_{0s}^2)Du_{0s}\right]\left(\alpha_0 k u_{0s} - \omega - i\alpha_0\gamma_{0s}^2 Du_{0s} - \frac{iu_{0s}}{2r_H}\right)\right.$$
$$-\frac{v_{Ts}^2}{2}\left[\alpha_0 k - \omega u_{0s} - \frac{i}{2r_H} - i\alpha_0\left(\frac{1}{n_{0s}}Dn_{0s} + 3\gamma_{0s}^2 u_{0s}Du_{0s}\right)\right]$$
$$\left.\times\left[\alpha_0 k - \omega u_{0s} - i\alpha_0\left(\frac{1}{P_{0s}}DP_{0s} - \frac{1}{n_{0s}}Dn_{0s}\right) - \frac{2i}{v_{Ts}^2}\left(1 + \frac{v_{Ts}^2}{2}\right)\left(\frac{1}{2r_H} + \alpha_0\gamma_{0s}^2 u_{0s}Du_{0s}\right)\right]\right\}^{-1}, \tag{22}$$

where $v_{Ts}^2 = 2\gamma_g\gamma_{0s}^2 P_{0s}/\rho_{0s}$ is the thermal velocity, u_{0s} is the radial component of the fluid velocity, and $\omega_{ps}^2 = 4\pi e^2\gamma_{0s}^2 n_{0s}^2/\rho_{0s}$ is the plasma frequency. Note that the plasma frequency is frame independent, that is, independent of γ_{0s} since the γ_{0s}^2 factor in the numerator cancels out the γ_{0s}^2 factor involved in the energy density, ρ_{0s}, in the denominator. The same is also true of the thermal velocity, for which the γ_{0s}^2 factors cancel.

The above dispersion relation is valid for either an electron-positron or an electron-ion plasma in that it makes no assumptions as to the mass, number density, or temperature of each species. In this respect it is completely general. If one considers the equivalent case to that of SK in [4] for an electron-positron plasma, in which the two fluids have the same velocity u_0, the same equilibrium density n_0, and are at the same temperature T_0, one obtains

$$1 = \frac{2\omega_p^2\alpha_0}{\gamma_0^2 k}\left[\alpha_0 k - \frac{i}{2r_H} - i\alpha_0\gamma_0^2\left(\frac{1}{n_0}Dn_0 + 2\gamma_0^2 u_0 Du_0\right)\right]$$
$$\times\left\{\left(\alpha_0 k u_0 - \omega - i\alpha_0\gamma_0^2\left(1+u_0^2\right)Du_0\right)\left(\alpha_0 k u_0 - \omega - i\alpha_0\gamma_0^2 Du_0 - \frac{iu_0}{2r_H}\right)\right.$$
$$-\frac{v_T^2}{2}\left[\alpha_0 k - \omega u_0 - \frac{i}{2r_H} - i\alpha_0\left(\frac{1}{n_0}Dn_0 + 3\gamma_0^2 u_0 Du_0\right)\right]$$
$$\left.\times\left[\alpha_0 k - \omega u_0 - i\alpha_0\left(\frac{1}{P_0}DP_0 - \frac{1}{n_0}Dn_0\right) - \frac{2i}{v_T^2}\left(1+\frac{v_T^2}{2}\right)\left(\frac{1}{2r_H} + \alpha_0\gamma_0^2 u_0 Du_0\right)\right]\right\}^{-1}. \quad (23)$$

If one now takes the limit of zero gravity so that $\alpha_0 \to 1$, the velocities $u_0 \to 0$, $\gamma_0 \to 1$ and the derivatives of the unperturbed quantities are set to zero,

$$Du_0 = Dn_0 = Dp_0 = DB_0 = 0\,,$$

the SK result is recovered,

$$\omega^2 = (2\omega_p^2 + k^2\gamma_g P_0/\rho_0)\,, \quad (24)$$

the only difference being that γ_g has been set to unity in the SK work.

V. NUMERICAL SOLUTION OF MODES

To determine all the physically meaningful modes for the longitudinal waves it is necessary to solve the dispersion relation given above numerically as was done for the transverse waves in paper I. The numerical procedure used has been described in paper I but is restated here for completeness. The roots of the dispersion relation have been determined using the well-known EISPACK routines based on the standard eigenvalue method [11]. The EISPACK routines require the wave equations to be supplied in the form of a matrix equation as

$$(A - kI)\,X = 0\,, \quad (25)$$

where the eigenvalue is chosen here to be the wave number k, the eigenvector X is given by the relevant set of perturbations, and I is the identity matrix. The vector A is the sum of two matrices A_R and A_I. The elements of these are, respectively, the real and imaginary terms in the coefficients of the equations for the perturbations.

The perturbation equations for the longitudinal waves must therefore be written in an appropriate form. The equations are conveniently expressed in terms of the following set of dimensionless variables:

$$\tilde{\omega} = \frac{\omega}{\alpha_0\omega_*}\,,\quad \tilde{k} = \frac{kc}{\omega_*}\,,\quad k_H = \frac{1}{2r_H\omega_*}\,,$$
$$\delta\tilde{u}_s = \frac{\delta u_s}{u_{0s}}\,,\quad \delta\tilde{n}_s = \frac{\delta n_s}{n_{0s}}\,,\quad \delta\tilde{E}_z = \frac{\delta E_z}{B_0}\,, \quad (26)$$

where ω_* is defined as $\omega_* = \omega_p = \sqrt{\omega_{p1}\omega_{p2}}$. Although δu_s and u_{0s} are already dimensionless, it is convenient to define $\delta\tilde{u}_s$ as above for consistency. The dimensionless eigenvector for the longitudinal set of equations is given by

$$\tilde{X}_{\text{longitudinal}} = \begin{bmatrix} \delta\tilde{u}_1 \\ \delta\tilde{u}_2 \\ \delta\tilde{n}_1 \\ \delta\tilde{n}_2 \\ \delta\tilde{E}_z \end{bmatrix}. \quad (27)$$

The equations leading to the dispersion relation for the longitudinal modes, Eqs. (18), (20), and (21), are rewritten in the appropriate dimensionless form as follows. The k-dependent term in the coefficient of δn_s in Eq. (18) is eliminated by substituting from Eq. (21) and, similarly, the k-dependent term in the coefficient of δu_s in Eq. (21) is eliminated by back substitution from Eq. (18). In terms of the dimensionless variables given by Eq. (26), Eqs. (18), (20), and (21) become

$$\tilde{k}\delta\tilde{u}_s = \frac{1}{u_{0s}^2 - v_{Ts}^2/2}\left\{u_{0s}\tilde{\omega}\left(1 - \frac{v_{Ts}^2}{2}\right) - i\left[\frac{k_H}{\alpha_0}\frac{v_{Ts}^2}{2} + \frac{v_{Ts}^2}{2}\frac{D\tilde{n}_{0s}}{n_{0s}} - u_{0s}\gamma_{0s}^2\left(1 + u_{0s}^2 - \frac{3v_{Ts}^2}{2}\right)D\tilde{u}_{0s}\right]\right\}\delta\tilde{u}_s$$
$$-\frac{1}{\gamma_{0s}^2}\frac{1}{(u_{0s}^2 - v_{Ts}^2/2)}\left\{\frac{v_{Ts}^2\omega}{2u_{0s}\gamma_{0s}^2} - i\left[\frac{k_H}{\alpha_0} + \left(u_{0s}^2\gamma_{0s}^2 - \frac{v_{Ts}^2}{2}\right)\frac{D\tilde{u}_{0s}}{u_{0s}} + \frac{v_{Ts}^2}{2}\left(\frac{D\tilde{P}_{0s}}{P_{0s}} - \frac{D\tilde{n}_{0s}}{n_{0s}}\right)\right]\right\}\delta\tilde{n}_s$$
$$-\frac{i(q_s/e)w_{cs}}{\gamma_{0s}^2\omega_p(u_{0s}^2 - v_{Ts}^2/2)}\delta\tilde{E}_z\,, \quad (28)$$

$$\tilde{k}\delta\tilde{n}_s = \frac{1}{u_{0s}^2 - v_{Ts}^2/2}\left\{u_{0s}\tilde{\omega}\left(1 - \frac{v_{Ts}^2}{2}\right) - i\left[\frac{k_H}{\alpha_0}\left(1 - u_{0s}^2 + \frac{v_{Ts}^2}{2}\right) + u_{0s}\gamma_{0s}^2\frac{v_{Ts}^2}{2}D\tilde{u}_{0s} + \frac{v_{Ts}^2}{2}\left(\frac{D\tilde{P}_{0s}}{P_{0s}} - \frac{D\tilde{n}_{0s}}{n_{0s}}\right)\right]\right\}\delta\tilde{n}_s$$
$$-\frac{u_{0s}^2\gamma_{0s}^2}{u_{0s}^2 - v_{Ts}^2/2}\left\{\frac{\tilde{\omega}}{u_{0s}\gamma_{0s}^2} - i\left[\frac{k_H}{\alpha_0} + \frac{D\tilde{n}_{0s}}{n_{0s}} + \gamma_{0s}^2\left(2u_{0s}^2 - 1\right)\frac{D\tilde{u}_{0s}}{u_{0s}}\right]\right\}\delta\tilde{u}_s + i\left(\frac{q_s}{e}\right)\frac{w_{cs}}{\omega_p\left(u_{0s}^2 - v_{Ts}^2/2\right)}\delta\tilde{E}_z, \quad (29)$$

and

$$\tilde{k}\delta\tilde{E}_z = iu_{01}^2\gamma_{01}^2\frac{\omega_{p1}^2}{\omega_{c1}\omega_p}\delta\tilde{u}_1 - iu_{02}^2\gamma_{02}^2\frac{\omega_{p2}^2}{\omega_{c2}\omega_p}\delta\tilde{u}_2 + i\frac{\omega_{p1}^2}{\omega_{c1}\omega_p}\delta\tilde{n}_1 - i\frac{\omega_{p2}^2}{\omega_{c2}\omega_p}\delta\tilde{n}_2\,. \tag{30}$$

These equations are now in the required form for use in the matrix equation, Eq. (25).

The derivatives of the equilibrium quantities, given by Eqs. (13), (14), and (19), are also expressed in terms of k_H so that

$$\left.\frac{dv_{\rm ff}}{dz}\right|_{\alpha=\alpha_0} \rightarrow -\frac{\alpha_0 k_H}{v_{\rm ff}} \tag{31}$$

and

$$D\tilde{u}_{0s} = -\frac{\alpha_0 k_H}{v_{\rm ff}}\,,\quad D\tilde{B}_0 = -\frac{4\alpha_0 k_H}{v_{\rm ff}^2}B_0\,,$$
$$D\tilde{n}_{0s} = -\frac{3\alpha_0 k_H}{v_{\rm ff}^2}n_{0s}\,,\quad D\tilde{P}_{0s} = -\frac{3\alpha_0 k_H\gamma_g}{v_{\rm ff}^2}P_{0s}\,. \tag{32}$$

VI. TWO-STREAM INSTABILITY

A. Introduction

The two-stream instability problem in the vicinity of a black hole is a difficult one, even allowing for the fact that the 3 + 1 formalism does lead to its own simplifications. The 3 + 1 formalism introduces problems in the choosing of an appropriate reference frame. In the special relativistic case investigated by Cornish [10], a clever choice of reference frame leads to an elegant and simplified treatment of the problem. Unfortunately, the power of the 3 + 1 formalism lies in the use of a preferred frame, the FIDO frame, which means that choosing a reference frame in which the fluid velocities are measured as purely counterstreaming velocities is no longer a desirable option. In the region near the horizon, the FIDO observer would see the two counterstreaming fluids falling in towards the horizon at different velocities. It is not unreasonable to assume that the FIDO observes both fluids falling in at the freefall velocity with an additional counterstreaming velocity component in the same radial direction. An observer in the FFO (freely falling frame) would view the fluids as having purely counterstreaming velocities. It is this frame which would then correspond to the frame chosen by Cornish in the special relativistic case.

The electrons and positrons (ions) are chosen to have counterstreaming velocities of magnitude v_0 in the z direction and a freefall velocity, $v_{\rm ff} = \left(1-\alpha^2\right)^{1/2}$, onto the black hole. Adding these relativistic velocities, the net radial velocity for each species, as viewed by a FIDO, is given by

$$\mathbf{v}_{0s} = \frac{v_{\rm ff} + \eta_s v_0}{1 + \eta_s v_0 v_{\rm ff}}\,\mathbf{e}_{\hat{z}}\,, \tag{33}$$

where

$$\eta_s = \begin{cases} -1\,, & s = 1, \\ +1\,, & s = 2\,. \end{cases}$$

Therefore, as measured by a FIDO, the net fluid velocities will approach unity at the horizon. This would imply that, as the fluids approach the horizon, any streaming phenomena would gradually die off. This is correct especially when considering that streaming phenomena were also found by Cornish to disappear for relativistic fluid speeds approaching c. The motion of the fluids is restricted to the radial direction and the **B** field is also taken to be in the radial z direction. Apart from being a realistic approximation to the field configuration in a region close to the horizon, this also ensures that the background magnetic field has no effect on the final result.

The dispersion relation for the two-stream instability in the vicinity of a Schwarzschild black hole, in the mean-field approximation, is derived from the linearized and Fourier transformed two fluid equations, namely from Eqs. (18), (20), and (21) where the terms involving the transverse perturbation terms are set to zero and u_{0s} and δu_s are replaced by v_{0s} and δv_s, respectively. Being a solution for longitudinal waves, the dispersion relation is exactly the one given for longitudinal waves above, Eq. (22), a completely general result as given. The difference now is that the velocities are different, thereby causing the equilibrium fluid quantities and their derivatives to be more complicated. The result is therefore more complicated than for the special relativistic case because cancellation of the Lorentz factors is no longer possible. The magnitudes of the net fluid velocities are no longer equal, thereby resulting in a different relativistic γ_{0s} for each species.

B. Dependence of equilibrium quantities on z

1. *Unperturbed fluid quantities*

The unperturbed fluid quantities and their respective derivatives are more complicated for the case where the fluid components are streaming through each other. The unperturbed radial velocity, for each fluid species, is no longer simply the freefall velocity, $v_{\rm ff}$, as for the longitudinal wave modes. This drastically changes the z dependence of all the equilibrium fluid quantities and means that they can no longer be set equal for the two fluid species, even when considering a counterstreaming electron-positron plasma, in which case both species would have the same rest mass and temperature.

The number density, for example, is no longer given by Eq. (9). Recall that the conservation law for the rest mass accretion rate (in the case of spherical, steady-state, adiabatic accretion onto a Schwarzschild black hole) states

that $r_H^2 n_{Hs} v_{Hs} = r^2 \alpha \gamma_{0s} n_{0s} v_{0s}$. Since $v_{\rm ff} = (r_H/r)^{\frac{1}{2}}$, the number density becomes

$$n_{0s}(z) = n_{Hs} \frac{v_{\rm ff}^4(z)}{\alpha \gamma_{0s} v_{0s}(z)} . \tag{34}$$

Similarly, the unperturbed pressure follows, as above, to become

$$P_{0s}(z) = P_{Hs} \frac{v_{\rm ff}^{4\gamma_g}(z)}{[\alpha \gamma_{0s} v_{0s}(z)]^{\gamma_g}} . \tag{35}$$

2. Derivatives of equilibrium quantities

The derivatives of the unperturbed quantities are, therefore, more complicated, given the more complex nature of the fluid velocities, as defined by Eq. (33). If the streaming velocity is chosen to be given by some fraction of the freefall velocity then, using the derivative of the freefall velocity, given by Eq. (13), the derivatives of the unperturbed fluid quantities can be written as

$$\left.\frac{1}{v_{0s}}\frac{dv_{0s}}{dz}\right|_{\alpha=\alpha_0} = -\frac{\alpha_0}{2r_H v_{\rm ff}} \frac{1-\eta_s v_0 v_{\rm ff}}{1+\eta_s v_0 v_{\rm ff}} ,$$

$$\left.\frac{1}{n_{0s}}\frac{dn_{0s}}{dz}\right|_{\alpha=\alpha_0} = -\frac{\alpha_0}{2r_H v_{\rm ff}^2} \frac{3-4v_0^2}{1-v_0^2} , \quad \text{and} \quad \left.\frac{1}{P_{0s}}\frac{dP_{0s}}{dz}\right|_{\alpha=\alpha_0} = \left.\frac{\gamma_g}{n_{0s}}\frac{dn_{0s}}{dz}\right|_{\alpha=\alpha_0} . \tag{36}$$

If, on the other hand, the streaming velocity is chosen to be a constant then the derivatives are given by

$$\left.\frac{1}{v_{0s}}\frac{dv_{0s}}{dz}\right|_{\alpha=\alpha_0} = -\frac{\alpha_0}{2r_H v_{\rm ff}} \frac{1-v_0^2}{v_{\rm ff}+\eta_s v_0} ,$$

$$\left.\frac{1}{n_{0s}}\frac{dn_{0s}}{dz}\right|_{\alpha=\alpha_0} = -\frac{\alpha_0}{2r_H v_{\rm ff}^2} \frac{3v_{\rm ff}+4\eta_s v_0}{v_{\rm ff}+\eta_s v_0} , \quad \text{and} \quad \left.\frac{1}{P_{0s}}\frac{dP_{0s}}{dz}\right|_{\alpha=\alpha_0} = \left.\frac{\gamma_g}{n_{0s}}\frac{dn_{0s}}{dz}\right|_{\alpha=\alpha_0} . \tag{37}$$

It is clear from Eqs. (36) and (37) that, in the limit as $\alpha \to 0$, the derivatives of the unperturbed fluid quantities become zero, as expected.

C. Dispersion relation

The dispersion relation is given by Eq. (22) but now v_{0s} replaces u_{0s} and Dv_{0s}, Dn_{0s} and DP_{0s} are defined in Eq. (19) but are evaluated using the derivatives given by Eq. (36) or Eq. (37). It is quoted here again:

$$\begin{aligned} 1 = \frac{\alpha_0}{k} \sum_s \frac{\omega_{ps}^2}{\gamma_{0s}^2} & \left[\alpha_0 k - \frac{i}{2r_H} - i\alpha_0 \gamma_{0s}^2 \left(\frac{1}{n_{0s}} Dn_{0s} + 2\gamma_{0s}^2 v_{0s} Dv_{0s}\right)\right] \\ \times & \left\{ \left(\alpha_0 k v_{0s} - \omega - i\alpha_0 \gamma_{0s}^2 \left(1+v_{0s}^2\right) Dv_{0s}\right) \left(\alpha_0 k v_{0s} - \omega - i\alpha_0 \gamma_{0s}^2 Dv_{0s} - \frac{i v_{0s}}{2r_H}\right) \right. \\ & - \frac{v_{Ts}^2}{2} \left[\alpha_0 k - \omega v_{0s} - \frac{i}{2r_H} - i\alpha_0 \left(\frac{1}{n_{0s}} Dn_{0s} + 3\gamma_{0s}^2 v_{0s} Dv_{0s}\right)\right] \\ \times & \left. \left[\alpha_0 k - \omega v_{0s} - i\alpha_0 \left(\frac{1}{P_{0s}} DP_{0s} - \frac{1}{n_{0s}} Dn_{0s}\right) - \frac{2i}{v_{Ts}^2} \left(1+\frac{v_{Ts}^2}{2}\right) \left(\frac{1}{2r_H} + \alpha_0 \gamma_{0s}^2 v_{0s} Dv_{0s}\right)\right]\right\}^{-1} . \end{aligned} \tag{38}$$

Although it is a completely unrealistic case, for an electron-positron plasma at zero temperature set $T_{0s} = 0$ for both species so that $v_{Ts}^2 = 0$ and the dispersion relation becomes

$$1 = \frac{\alpha_0}{k} \sum_s \frac{\omega_{ps}^2}{\gamma_{0s}^2} \frac{[\alpha_0 k - i/2r_H - i\alpha_0 \gamma_{0s}^2 (Dn_{0s}/n_{0s} + 2\gamma_{0s}^2 v_{0s} Dv_{0s})]}{[\alpha_0 k v_{0s} - \omega - i\alpha_0 \gamma_{0s}^2 (1+v_{0s}^2) Dv_{0s}][\alpha_0 k v_{0s} - \omega - i\alpha_0 \gamma_{0s}^2 Dv_{0s} - i v_{0s}/2r_H]} . \tag{39}$$

Unlike the special relativistic case, the densities and therefore also the plasma frequencies remain different for each species because of the different velocities and hence different relativistic γ_{0s} factors.

As for the longitudinal and tranverse electromagnetic modes, already treated, the two stream modes must be found by solving for the roots of the dispersion relation numerically. The equations required to do this are simply those for the longitudinal modes, given by Eqs. (28)–(30). The only difference is that now u_{0s} is replaced by v_{0s} and the equilibrium field and fluid quantities take on the values given by Eqs. (34)–(37).

VII. RESULTS

Although both the electron-positron and electron-ion cases are considered for the longitudinal waves, only the electron-positron results are discussed for the two-stream instability. This is because it is far more likely for counterstreaming electron and positron fluids to exist in the environment close to the black hole horizon [12]. Also, the results are expected to be similar for both cases. The limiting horizon values for the magnetic field and the fluid parameters are as follows. For the electron-positron plasma the horizon values are chosen to be

$$n_{Hs} = 10^{18}\ \mathrm{cm}^{-3},\quad T_{Hs} = 10^{10}\ \mathrm{K},\quad B_H = 3\times 10^6\ \mathrm{G}\,. \tag{40}$$

For the electron-ion plasma the limiting values are chosen to be

$$\begin{aligned} n_{H1} &= 10^{18}\ \mathrm{cm}^{-3},\quad T_{H1} = 10^{10}\ \mathrm{K},\\ n_{H2} &= 10^{15}\ \mathrm{cm}^{-3},\quad T_{H2} = 10^{12}\ \mathrm{K}\,. \end{aligned} \tag{41}$$

The limiting horizon value for the equilibrium magnetic field takes on the same value as it does for the electron-positron case above. For both cases the gas constant and the mass of the black hole have been chosen to be

$$\gamma_g = \frac{4}{3}\ \text{and}\ M = 5M_\odot\,.$$

A. Longitudinal modes

It is for the longitudinal waves that the transonic radius begins to play a significant role. From Eqs. (28) and (29) it is clear that there occurs a singularity at the point for which the infall (in this case, freefall) velocity equals the fluid thermal velocity, $u_{0s}^2 = v_{Ts}^2$. The position of the transonic radius for each fluid is principally dependent on the fluid temperature, in this case the limiting temperature of each fluid at the horizon, which determines the temperature at any given radius. One would expect, therefore, that the transonic radius for each fluid should manifest itself in some way in the results and this is borne out by what follows. This singularity is not dependent in any way on the accretion model adopted but rather is a direct consequence of the fluid equations themselves.

1. Electron-positron plasma

The longitudinal modes are split into high and low frequency domains, distinguished by $\tilde{\omega} < \sqrt{2}$ and $\tilde{\omega} > \sqrt{2}$. There exist four modes in both the high and low frequency domains. This is in contrast with the special relativistic case investigated by SK where only one high frequency mode was found to exist for the electron-positron plasma, as illustrated in Fig. 1.

The first low frequency mode, Fig. 2, is only physical for $\alpha_0 < \alpha_t$, where α_t denotes the transonic radius, which occurs at about $\alpha_t \sim 0.86$ for the case considered here.

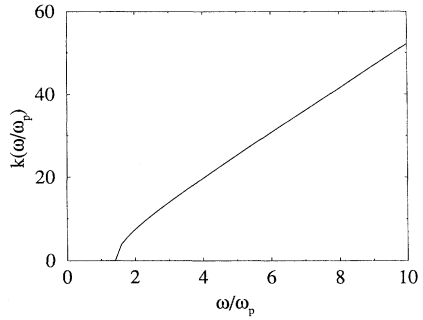

FIG. 1. Special relativistic result of SK for the high frequency longitudinal mode for an ultrarelativistic electron-positron plasma. The fluid and field parameters were chosen to be $n_0 = 10^{15}\,\mathrm{cm}^{-3}$, $T_0 = 10^9$ K, $B_0 = 3\times 10^4$ G, and $\gamma_g = 4/3$.

This mode is odd in that there appears to be some interplay between frequency and distance from the horizon, denoted by α_0, which splits this mode into two distinct regions, one of almost pure growth for which $\mathrm{Im}(k) \gg \mathrm{Re}(k)$ and the other which is also a growth region but where $\mathrm{Im}(k) \ll \mathrm{Re}(k)$. The "ridge" dividing these two regions is where $\mathrm{Im}(k) \ll 0$. The second mode, Fig. 3, is also physical for $\alpha_0 < \alpha_t$ but is damped for most of the low frequency domain but becomes a growth mode as $\alpha_0 \to 0$. The third mode (not illustrated) is damped for $\alpha_0 < \alpha_t$ but growing for $\alpha_0 > \alpha_t$. Of course, the region of interest is mainly for $\alpha_0 < \alpha_t$ so that this mode can be regarded as a damped mode. This means that energy is drained from the wave rather than being fed into it by the gravitational field. The fourth and final mode (also not shown here) is a growth mode for the whole low frequency and α_0 domain.

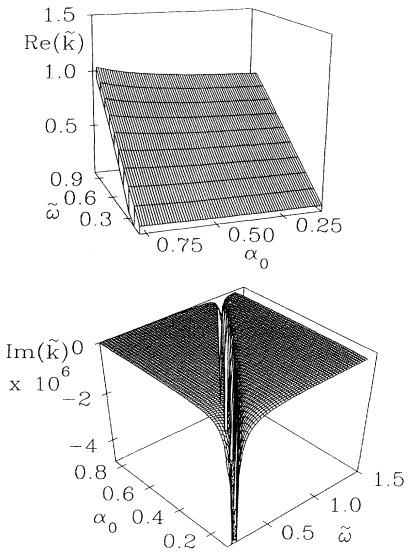

FIG. 2. Longitudinal low frequency mode for the electron-positron plasma.

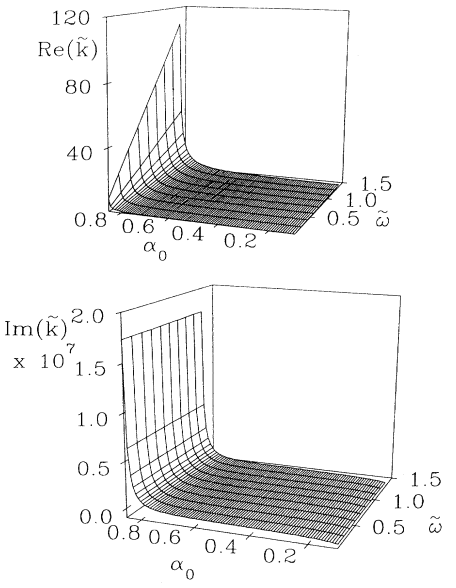

FIG. 3. Longitudinal low frequency mode for the electron-positron plasma.

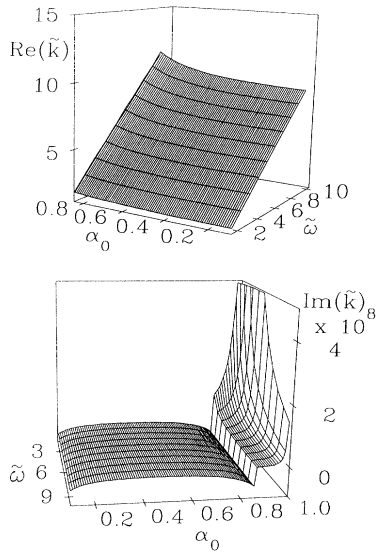

FIG. 5. Longitudinal high frequency mode for the electron-positron plasma.

In the high frequency domain there also exist four modes. The first two (only one of these is depicted in Fig. 4) are damped for $\alpha_0 < \alpha_t$, although they are growing for $\alpha_0 > \alpha_t$. Again, energy is being drained from the waves rather than being fed into them by the gravitational field. The other two modes are both growth modes for $\alpha_0 < \alpha_t$, although the last of these, shown in Fig. 5, is damped above α_t.

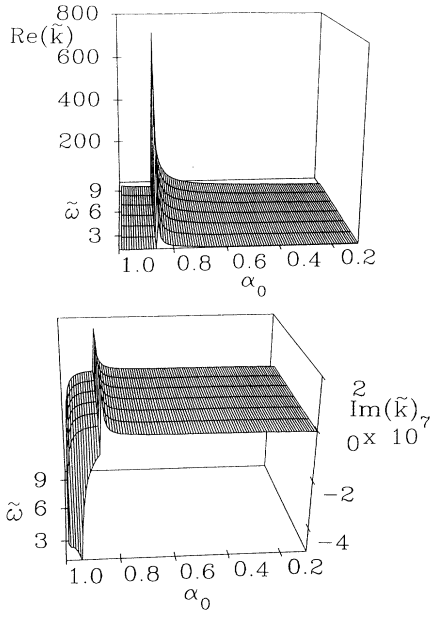

FIG. 4. Longitudinal high frequency mode for the electron-positron plasma.

2. *Electron-ion plasma*

The two frequency domains are distinguished here by $\tilde{\omega} < 1$ and $\tilde{\omega} > 1$. As for the electron-positron case, there exist four low frequency modes. In this case, however, the fluids are at different temperatures and so their transonic radii, α_t, will be different. The transonic radius for the electrons is the same as for the electron-positron case and occurs at about $\alpha_{t1} \sim 0.84$. The transonic radius for the ions, however, occurs outside the range of α_0 shown here, therefore $\alpha_{t2} \gtrsim 0.99$.

The first low frequency mode, Fig. 6, shows the tran-

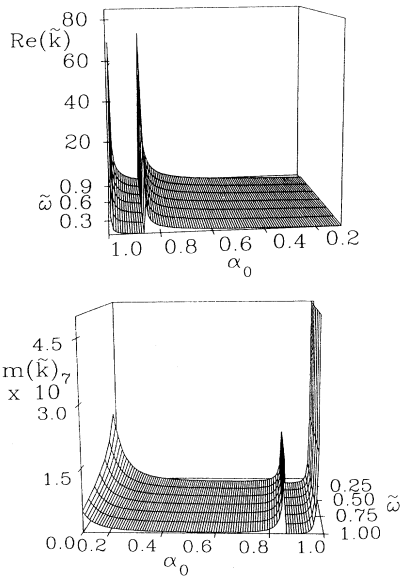

FIG. 6. Longitudinal low frequency mode for the electron-ion plasma.

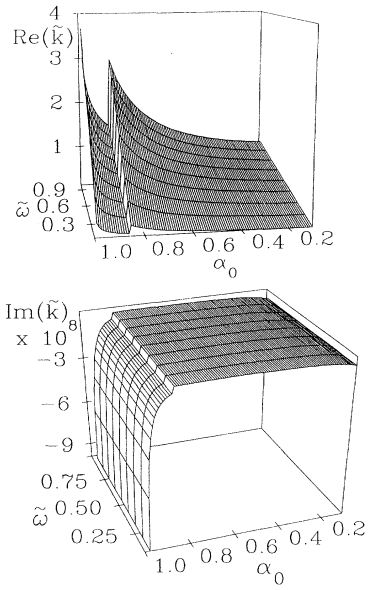

FIG. 7. Longitudinal low frequency mode for the electron-ion plasma.

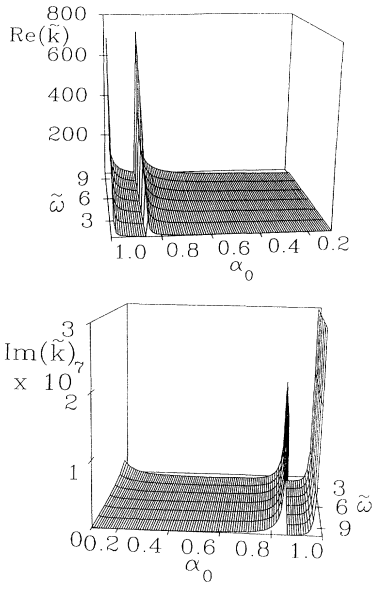

FIG. 9. Longitudinal high frequency mode for the electron-ion plasma.

sonic radii clearly. This mode is growing for $\alpha_0 > \alpha_{t1}$ but damped for $\alpha_0 < \alpha_{t1}$. It is also damped above α_{t1} very close to α_{t2}. This is interesting as, again, energy is being fed into the wave between the transonic radii but is drained from the wave very close to the horizon. The second mode (not shown) is a growth mode. This mode corresponds to the electron-positron mode shown in Fig. 2 and appears to be insensitive to both α_{t1} and α_{t2}. Again, there is some interplay between frequency, $\tilde{\omega}$ and α_0 causing the characteristic "ridge" along which the singularity occurs. The third mode (not illustrated) is only physical for $\alpha_0 < \alpha_{t1}$ and is a growth mode in this region. The fourth mode, Fig. 7, is physical over the whole domain and is also a growth mode although the growth rate is greater for $\alpha_{t1} < \alpha_0 < \alpha_{t2}$ than for $\alpha_0 < \alpha_{t1}$.

In the high frequency domain there are also four branches, as with the electron-positron plasma. The first of these, Fig. 8, is physical only for $\alpha_0 < \alpha_{t1}$ and is the high frequency continuation of the third low frequency mode (not shown). It is also a growth mode. The second high frequency mode, Fig. 9, shows the effects of the transonic radii quite clearly. It is a growth mode in the region between α_{t1} and α_{t2} but is damped as $\alpha_0 \to \alpha_{t2}$

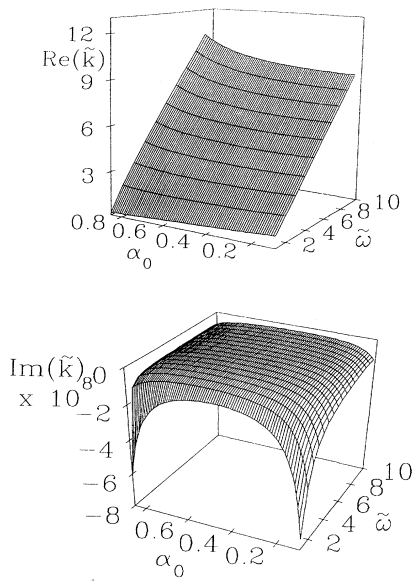

FIG. 8. Longitudinal high frequency mode for the electron-ion plasma.

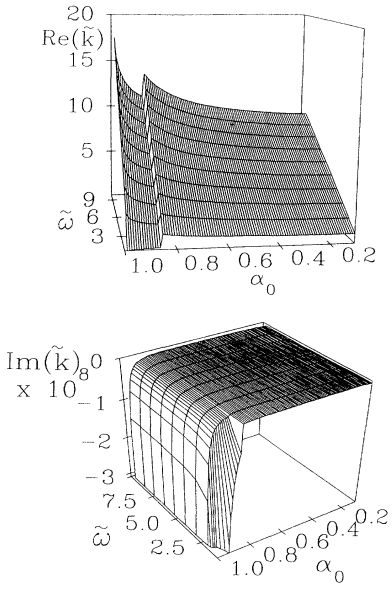

FIG. 10. Longitudinal high frequency mode for the electron-ion plasma.

and for $\alpha_0 < \alpha_{t1}$. Again, this is a case of energy being drained from the wave into the gravitational field closer to the horizon. The third mode (not illustrated) is a growth mode over the whole frequency and α_0 domain. The transonic radii are again clearly evident, and the growth rate is greater for $\alpha_0 > \alpha_{t1}$ as it is in Fig. 7. The fourth mode, Fig. 10, also clearly shows the influence of the transonic radii and is a growth mode. As for the previous mode, the growth rate is greater for $\alpha_0 > \alpha_{t1}$ and especially as $\tilde{\omega} \to 0.99$. As in the electron-positron case there is no high frequency equivalent to the second low frequency mode for the electron-ion plasma.

B. Two-stream instability

For the two-stream instability two cases are considered. First, the case for a relatively small streaming velocity (i.e., small compared with the freefall velocity, $v_{\rm ff}$) and second, the case for a high streaming velocity. Only the electron-positron plasma is dealt with here as the electron-ion plasma yields similar results (as in the case of the longitudinal waves with no streaming).

1. Case: Low streaming velocity

In this case, the streaming velocity is chosen to be $v_0 = 0.25 v_{\rm ff}$. As for the longitudinal waves, both the low and high frequency domains are discussed. Since now the velocities are different for each species, the transonic radii for the two species will be shifted in opposite directions.

In the low frequency domain there exist four branches as for the longitudinal modes. The first of these (not illustrated) is only physical for $\alpha_0 < \alpha_{t1}$, where α_{t1} denotes the transonic radius for the electrons and occurs at $\alpha_{t1} \sim 0.78$. In this region it is a growth mode for all frequencies. The second mode (also not shown) is physical for all α_0 and all frequencies except for very low frequencies, $\tilde{\omega} \lesssim 0.2$. In this region $\mathrm{Re}(k)$ is negative but $|\mathrm{Re}(k)| \ll 1$. This mode is a growth mode and appears to be insensitive to the transonic points. It corresponds to the longitudinal low frequency mode in Fig. 2. The third mode, Fig. 11, is physical for $\alpha_0 < \alpha_{t2}$, where $\alpha_{t2} \sim 0.91$ and denotes the transonic radius for the positron fluid. This mode is a growth mode for $\alpha_{t1} < \alpha_0 < \alpha_{t2}$ but is damped for $\alpha_0 < \alpha_{t2}$ until about $\alpha_0 \sim 0.3$, below which it again shows growth. The growth rate close to the horizon

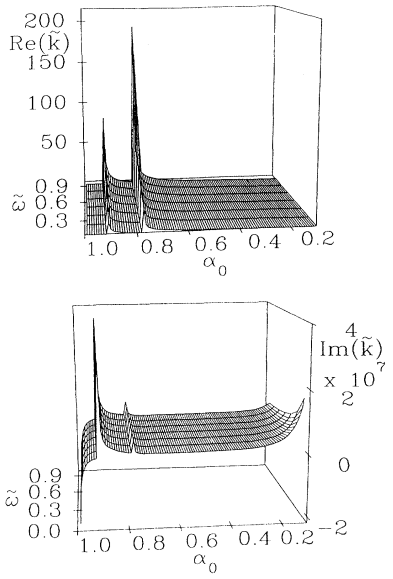

FIG. 12. High frequency mode for the electron-positron plasma with $v_0 = 0.25 v_{\rm ff}$.

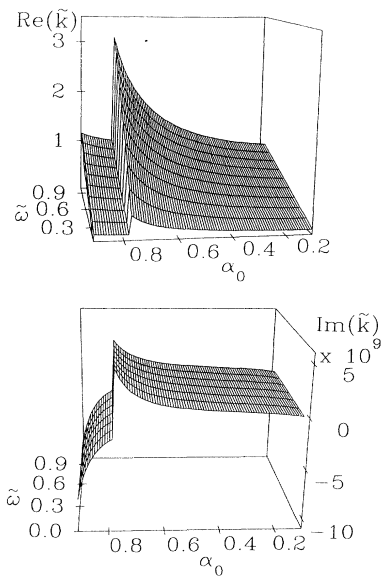

FIG. 11. Low frequency mode for the electron-positron plasma with $v_0 = 0.25 v_{\rm ff}$.

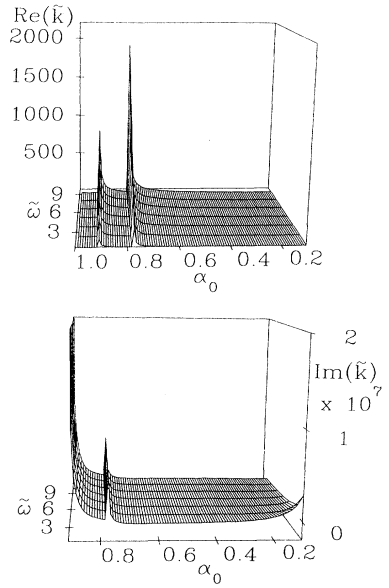

FIG. 13. High frequency mode for the electron-positron plasma with $v_0 = 0.25 v_{\rm ff}$.

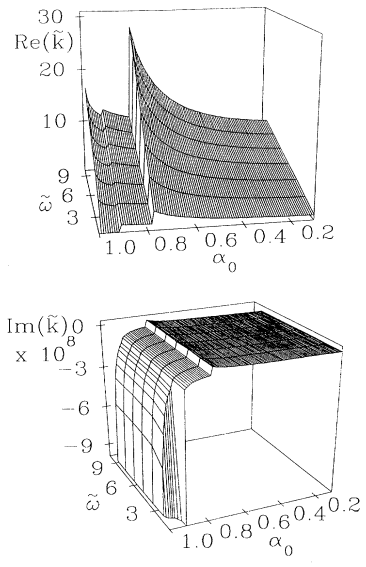

FIG. 14. High frequency mode for the electron-positron plasma with $v_0 = 0.25 v_{ff}$.

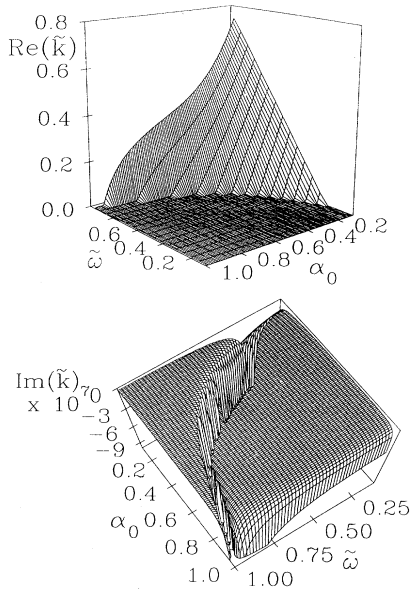

FIG. 15. Low frequency two-stream growth mode with $v_0 = 0.75 v_{ff}$.

is, however, much smaller than for $\alpha_{t1} < \alpha_0 < \alpha_{t2}$. The fourth branch, Fig. 12, is damped for $\alpha_{t1} < \alpha_0 < \alpha_{t2}$. Below α_{t1} however, it is damped for low frequencies but growing for higher frequencies approaching $\tilde{\omega} \to 1$. Very close to the horizon, however, it is damped at all frequencies.

Again, there are four high frequency modes in total, some of which are not physical over the entire α_0-$\tilde{\omega}$ plane. As for the longitudinal waves there is no mode corresponding to the low frequency mode shown in Fig. 2 in the high frequency range. The first mode (not illustrated) is a growth mode which is physical only for $\alpha_0 < \alpha_{t1}$. The growth rate is greatest for $\tilde{\omega} \to 1$. The second mode (also not shown) is also a growth mode which is physical for $\alpha_0 < \alpha_{t2}$. The third mode, Fig. 13, shows both damping and growth. It is damped for $\alpha_{t1} < \alpha_0 < \alpha_{t2}$ but becomes a growth mode below α_{t1}. As $\alpha_0 \to 0$, however, it is again damped for low frequencies, that is to say, for $\tilde{\omega} \to 1$. The fourth mode, Fig. 14, is almost the opposite of the previous mode in that it is a growth mode for $\alpha_{t1} < \alpha_0 < \alpha_{t2}$, is damped just below α_{t1} and then, for $\alpha_0 \lesssim 0.54$ it makes the transition back to growth.

2. *Case: High streaming velocity*

In this case, the streaming velocity is chosen to be $v_0 = 0.75 v_{ff}$. As expected, there are four modes for each of the low and high frequency domains. Because the difference between the net infall velocities of the two fluids, as measured by a FIDO, is now greater one would expect that the gap between the transonic radii would also be greater and that they would both be shifted in closer to the horizon. This is indeed borne out by the results that follow. It is found that the transonic radius for the electrons occurs now at $\alpha_{t2} \sim 0.96$ and for the positrons at $\alpha_{t1} \sim 0.46$.

The first low frequency mode (not illustrated here) is physical only for $\alpha_0 < \alpha_{t1}$ and is damped. Hence, again energy is being drained from the wave into the gravitational field of the black hole. The second mode, Fig. 15, corresponds to the longitudinal low frequency mode shown in Fig. 2. Unlike the corresponding mode in the case for a low streaming velocity, this mode is not physical over the entire α_0-$\tilde{\omega}$ plane but only in the region which

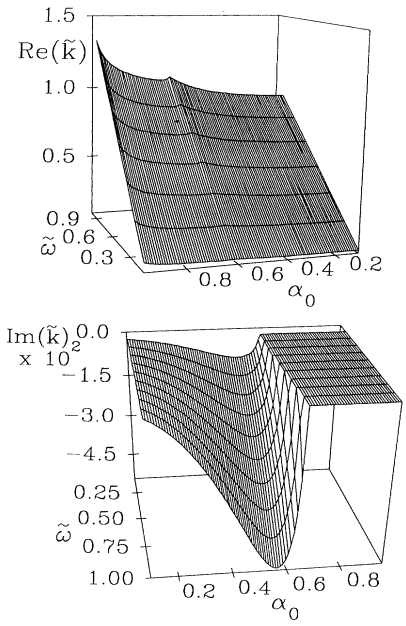

FIG. 16. Low frequency two-stream growth mode with $v_0 = 0.75 v_{ff}$.

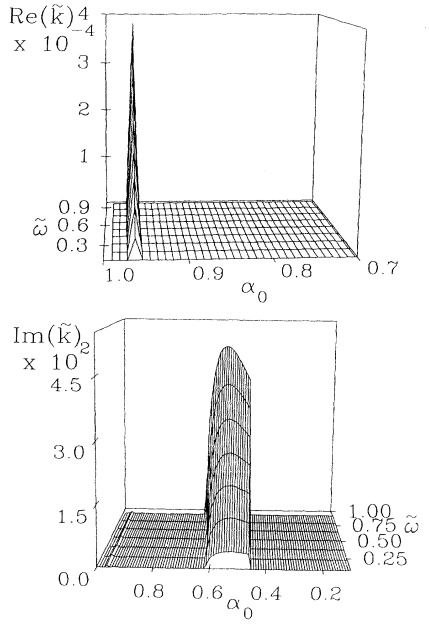

FIG. 17. Low frequency two-stream mode with $v_0 = 0.75v_{ff}$ showing both damping and growth for $\alpha_0 < \alpha_{t2}$.

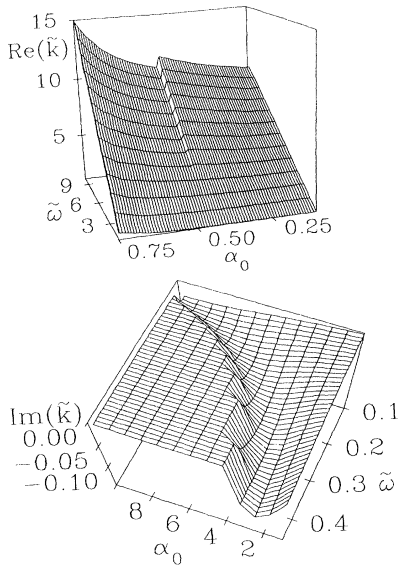

FIG. 19. High frequency two-stream mode with $v_0 = 0.75v_{ff}$ showing both damping and growth.

obviously shows $\mathrm{Re}(k) > 0$. Over the remainder of the region it is found that $\mathrm{Re}(k) < 0$ but also $|\mathrm{Re}(k)| \ll 1$. In the physically meaningful region the mode is growing, and the growth rate increases close to the boundary. The third mode, Fig. 16, is a growth mode and is physical for $\alpha_0 < \alpha_{t2}$. There is an interesting feature at about $\alpha_0 \sim 0.64$ which is unrelated to the transonic points. The fourth mode, Figs. 17 and 18, is damped for $\alpha_{t1} < \alpha_0 < \alpha_{t2}$ but becomes a growth mode below α_{t1}. At low frequencies, $\tilde{\omega} \to 0$ and for $\alpha_0 \to 0$, however, the mode again makes the transition to being damped.

The first high frequency mode (not shown) is physical for $\alpha_0 < \alpha_{t1}$ and is a growth mode in this region. The second mode, shown in Figs. 19 and 20, is a growth mode for $\alpha_0 > \alpha_{t2}$ but is damped for $\alpha_{t1} < \alpha_0 < \alpha_{t2}$ and then becomes a growth mode again for $\alpha_0 < \alpha_{t1}$, where $\alpha_{t2} \sim 0.96$ and $\alpha_{t1} \sim 0.46$. The third mode, Fig. 21, is only physical for $\alpha_0 < \alpha_{t2}$. It is a growth mode for $\alpha_{t1} < \alpha_0 < \alpha_{t2}$ but makes a transition to damping for $\alpha_0 < \alpha_{t1}$. The fourth mode, Fig. 22, is a growth mode

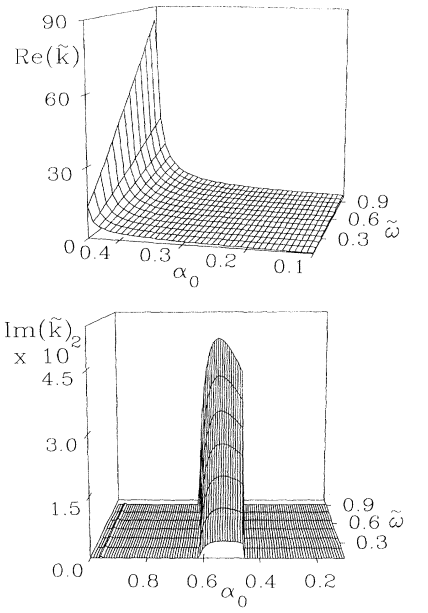

FIG. 18. Low frequency two-stream mode with $v_0 = 0.75v_{ff}$ showing both damping and growth for $\alpha_0 > \alpha_{t2}$.

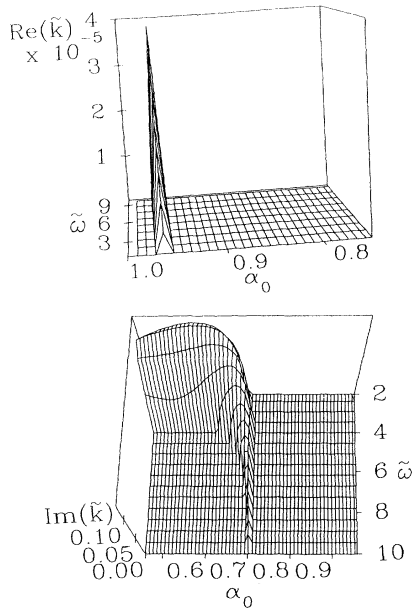

FIG. 20. High frequency two-stream mode with $v_0 = 0.75v_{ff}$ showing both damping and growth for $\alpha_0 > \alpha_{t2}$.

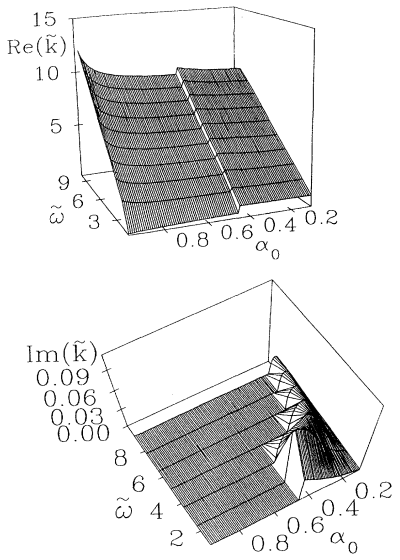

FIG. 21. High frequency two-stream mode with $v_0 = 0.75 v_{ff}$ showing both damping and growth.

everywhere except for low frequencies, $\tilde{\omega} \to 1$, as $\alpha_0 \to 0$.

From the preliminary results obtained here, a comparison of the longitudinal wave modes with no streaming and those including a counterstreaming component in the fluid velocities appears to indicate that the major difference between them is that the change in the radial position of the transonic radius of each fluid affects the regions in ω-α_0 space where the various modes become physical, that is, where $\mathrm{Re}(k) > 0$.

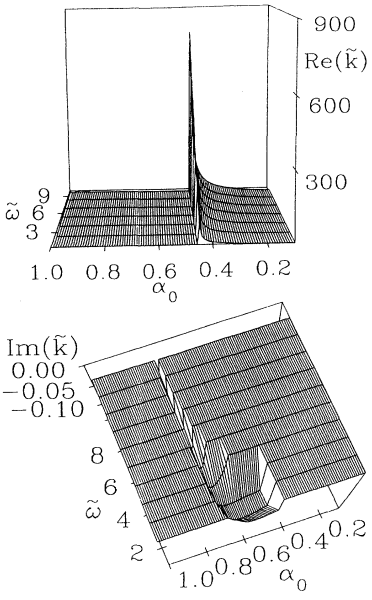

FIG. 22. High frequency two-stream mode with $v_0 = 0.75 v_{ff}$ showing both damping and growth.

VIII. CONCLUSION

Using a local approximation, the dispersion relation for the longitudinal waves and the two-stream instability has been derived. In the limit of zero gravity these results reduce, respectively, to the special relativistic results obtained by Sakai and Kawata [4] for the longitudinal waves and Cornish [10] for the two-stream instability.

One interesting point concerning the longitudinal waves in the electron-positron plasma is that, unlike the results found by SK for which only one high frequency mode exists, here there is no such restriction on the frequency and four low frequency modes are found, as with the electron-ion plasma. For both the electron-positron and electron–ion plasmas, a total of four low and four high frequency modes are found. Different modes become physical [$\mathrm{Re}(k) > 0$] at the boundaries defined by the transonic radius for each fluid. This is true for the majority of the modes, except for one intriguing low frequency mode, in both the electron-positron and electron-ion plasmas. For this mode some complicated interplay between frequency and radial distance appears to determine the regions in the ω-α_0 plane for which the mode is physical.

The results for the two-stream instability are very similar to those for the longitudinal waves. Because of the fact that the velocities for each fluid now contain a counterstreaming component, the transonic radii for the electron and positron fluids are different. This affects the regions in α_0 space for which the various modes are physical and to a large extent explains the difference between the results for the longitudinal waves and for the two-stream instability in the local approximation. As was also found in paper I, the fact that some modes are damped demonstrates that energy is being removed from some of the waves and transferred to the gravitational field. On the other hand, the majority of the modes exhibit growth rates indicating that the gravitational field is feeding energy into the waves.

The present paper complements the work on Alfvén and high frequency electromagnetic waves presented in paper I with the investigation of longitudinal waves and the two-stream instability in the two-fluid plasma surrounding a Schwarzschild black hole. Although the local approximation adopted in these two papers makes it possible to obtain dispersion relations describing the various wave modes at a range of fixed values of the lapse function, α, this does not lead to a realistic and complete description of the linear wave modes. In order to investigate such waves fully, a numerical solution of the linearized two fluid equations is necessary, with appropriate boundary conditions at radial infinity, to obtain the velocity, density, and field perturbations as functions of the radial coordinate. This has been carried out and leads, amongst other things, to a determination of the average electromagnetic energy density for each of the various waves. This is an example of the sort of information that can be obtained from a full treatment of the linear two fluid equations. These investigations will form the subject matter of a paper to follow.

ACKNOWLEDGMENTS

Support from DITAC and the ARC enabled two of the authors (V. Buzzi and K. C. Hines) to work at MPE, Garching and at the Università di Padova. V. Buzzi also acknowledges financial support from the Palladio Trust and APRA. We have received valuable advice on general relativity from R. Turolla and L. Nobili at the Università di Padova and on numerical techniques from L. Berge, now at Murdoch University, Western Australia.

[1] V. Buzzi, K. C. Hines, and R. A. Treumann, preceding paper, Phys. Rev. D **51**, 6663 (1995).

[2] K. S. Thorne and D. A. Macdonald, Mon. Not. R. Astron. Soc. **198**, 339 (1982); D. A. Macdonald and K. S. Thorne, *ibid.* **198**, 345 (1982); R. H. Price and K. S. Thorne, Phys. Rev. D **33**, 915 (1986).

[3] K. S. Thorne, R. H. Price, and D. A. Macdonald, *Black Holes: The Membrane Paradigm* (Yale University Press, New Haven, 1986).

[4] J. Sakai and T. Kawata, J. Phys. Soc. Jpn. **49**, 747 (1980).

[5] D. G. Lominadze and A. B. Mikhailovskii, Sov. Phys. JETP **49**, 483 (1979).

[6] P. Goldreich and W. H. Julian, Astrophys. J. **157**, 869 (1969).

[7] B. Buti, Phys. Fluids **6**, 89 (1962); **6**, 100 (1962).

[8] B. Buti, Phys. Rev. A **5**, 1558 (1972); **5**, 1846 (1972).

[9] D. Finkelstein and P. A. Sturrock, in *Plasma Physics*, edited by J. E. Drummond (McGraw-Hill, New York, 1961).

[10] N. Cornish, University of Melbourne, 4th Year report, 1989 (unpublished).

[11] J. Stoer and R. Bulirsch, trans. R. Bartels, W. Gautschi, and C. Witzgall, *Introduction to Numerical Analysis* (Springer-Verlag, New York, 1980).

[12] M. J. Rees, Annu. Rev. Astron. Astrophys. **22**, 471 (1984).